AIP | Applied Physics Letters

Self-accelerating parabolic beams in quadratic nonlinear media

Ido Dolev, Ana Libster, and Ady Arie

Citation: Appl. Phys. Lett. **101**, 101109 (2012); doi: 10.1063/1.4748979
View online: http://dx.doi.org/10.1063/1.4748979
View Table of Contents: http://apl.aip.org/resource/1/APPLAB/v101/i10
Published by the American Institute of Physics.

Self-accelerating parabolic beams in quadratic nonlinear media

Ido Dolev,[a] Ana Libster, and Ady Arie
Department of Physical Electronics, Fleischman Faculty of Engineering, Tel-Aviv University, Tel-Aviv 69978, Israel

(Received 21 May 2012; accepted 15 August 2012; published online 5 September 2012)

We present experimental observation of self-accelerating parabolic beams in quadratic nonlinear media. We show that the intensity peaks of the first and second harmonics are asynchronous with respect to one another in the two transverse coordinates. In addition, the two coupled harmonics have the same acceleration within and after the nonlinear medium. We also study the evolution of second harmonic accelerating beams inside the quadratic media and their correlation with theoretical beams. © *2012 American Institute of Physics*. [http://dx.doi.org/10.1063/1.4748979]

Self-accelerating optical beams are attracting a lot of interest since 30 years old ideas of self-accelerating quantum particles[1] were realized in the field of optics theoretically[2] and experimentally.[3,4] Ideally, these beams propagate in a parabolic trajectory ("accelerating" in the transverse plane as they propagate) without changing their shape. However, such beams carry infinite power, hence in reality the beams have to be truncated, usually by an exponential or Gaussian window. This implies that the beam can accelerate and approximately maintain its structure for a finite distance only, yet physically this distance can be very large (many diffraction lengths).[2,3] All of these features make these self-accelerating beams useful for a range of applications, e.g., manipulation of small particles,[5] generation of curved plasma channels in air,[6] generation of linear light bullets,[7,8] Airy beam lasers,[9,10] etc. Although Airy beams were the first to be experimentally observed,[3] another family of accelerating beams was presented by Bandres:[11] the accelerating parabolic beams. These beams have the same unusual properties as the Airy beams (i.e., they self accelerate and preserve their shape) but have an inherent parabolic geometry and are more localized compared with the Airy beams. In addition, together with the two-dimensional Airy beams, they are the only orthogonal and complete family of explicit solutions of the two dimensional paraxial wave equation that remain diffraction free and freely accelerate during propagation.[11] Several works were published on parabolic beams[11,12] and on general accelerating beams[13,14] all in linear medium (usually in free space); however, the interactions of these beams within a nonlinear medium have not been studied so far. In comparison, accelerating Airy beams where studied extensively within nonlinear media. Experiments with Airy beams in quadratic media include the generation and manipulation of Airy beams through engineered periodic poling,[15–17] and three-wave-mixing of Airy beams.[18–20] Recently, a theoretical prediction[21] followed by experimental observation[22] showed that quadratic nonlinearities can support self-accelerating self-trapped beams: accelerating beams comprised of a fundamental and second harmonic (SH) frequencies that propagate along a joint curved trajectory and are mutually trapped (by virtue of the nonlinearity) such that they exhibit shape-preserving propagation in the accelerated frame.

In this letter, we present experimental observations of self-accelerating nonlinearly generated parabolic beams in quadratic nonlinear media. We find that the unique phenomena that were predicted and observed for 1D and 2D Airy beam can be generalized in more complex form to the case of parabolic beams. Highlighting features such as intensity peaks of the first and second harmonics that are asynchronous with one another and mutual acceleration along a joint trajectory were experimentally observed. In the last part of this letter we study the correlation of the generated second harmonic beam and the theoretical shape-preserving beam as a function of the interaction length.

Let us begin with the theory. We will use the notation of Ref. 12 to describe parabolic beams:

$$\phi_n(\eta,\xi,z) = \exp[(z/2k\kappa^2 - ia)(\eta^2-\xi^2)/2] \cdot \exp[(z/2k\kappa^2 - ia)^3/3]\Theta_n(\eta)\Theta_n(i\xi), \quad (1)$$

where(η, ξ) are dimensionless parabolic coordinates defined with respect to the Cartesian transverse coordinates (x,y) as $[x/\kappa - (z/2k\kappa^2)^2 + iaz/k\kappa^2, y/\kappa] = (\eta^2/2 - \xi^2/2,\ \eta\xi)$, κ is a transverse scale, k is the wave number and the functions $\Theta_n(\eta)$ (where $n = 0, 1, 2,\ldots$) are the square integrable eigensolutions of the quartic oscillator equation.[23] a is the exponential decaying constant that is used to truncate the beam, so that it will carry finite energy.

Now moving to the quadratic nonlinear medium, as was done in Refs. 21 and 22, consider the paraxial phase-matched propagation of two coupled beams $\psi^{(1)}, \psi^{(2)}$ at the first and second harmonics, respectively, assuming the undepleted pump approximation

$$i\psi_z^{(2)} + \frac{1}{4k}\nabla_\perp^2\psi^{(2)} + 2k\mu\left(\psi^{(1)}\right)^2 = 0, \quad (2)$$

k is the first harmonic (FH) wave-number and μ is the effective nonlinear coupling coefficient between the first harmonic and second harmonic beams (proportional to $\chi^{(2)}$).

The solution for the case where $\psi^{(1)} \propto$: $Ai(x)$ was found using asymptotic and numerical methods[21] and was verified experimentally.[22] For 2D acceleration parabolic beams studied here, the solution can be found numerically for the

[a]Electronic mail: idodolev@post.tau.ac.il.

undepleted pump, $\psi^{(1)} \propto: \phi_n(\eta, \xi, z)$. As we will show below, the generated beam from a parabolic fundamental beam exhibits faster oscillations in the transverse coordinates, but jointly accelerates with the fundamental beam.

We now proceed to describe the experiments. In order to convert the fundamental Gaussian beam of the laser into a truncated parabolic beam, we designed and fabricated a binary phase hologram that generates the required parabolic beam at its first far field diffraction order. The hologram surface is given by[24]

$$h(x,y) = \frac{h_0}{2}\{1 + sign[\cos[2\pi/_\Lambda\, x - \varphi(x,y)] - \cos[\pi q(x,y)]]\}, \tag{3}$$

where h_0 is the grating's ridge height, Λ is the period of the hologram's carrier frequency and $\sin[\pi q(x,y)] = A(x,y)$. A(x, y) and φ(x, y) are the amplitude and the phase, respectively, of the Fourier transform (FT) of the desired wave front in the first diffraction order. A(x,y) is normalized to the range 0–1, and φ(x, y) is in the range 0–2π. In this case, $A(x,y)\exp[i\varphi(x,y)]$ is proportional to[25]

$$F[\phi_n](k_x, k_y) \propto \exp[i\kappa^3(k_x^3/3 - a^2 k_x/\kappa^2 + k_x k_y^2)] \times \exp[-a\kappa^2(k_x^2 + k_y^2)]\Theta_n(\sqrt{2}k_y\kappa) \tag{4}$$

and the desired beam, $\phi(\eta, \xi) \propto FT\{A(x,y)\exp[i\varphi(x,y)]\}$, is obtained at the first far-field diffraction order. In order to obtain a parabolic beam, a lens is used to Fourier transform the wave at the first diffraction order.

We fabricated the phase masks by evaporating 20 nm chromium layer (required for good adhesion of the successive metal layers to the wafer), followed by 70 nm of gold layer, both of them on top of a silicon wafer. This was then followed by a standard e-beam lithography technique to print the desired structure on a polymethyl methacrylate (PMMA) mask. A 245 nm gold layer (which provides the optimal phase difference of π, when the fundamental beam at 1.0475 μm is sent at an angle of 20°) was then evaporated on top of the patterned PMMA, followed by immersion of the sample in acetone which lifted-off the PMMA and the gold metal layer on top of it. The result was a 245 nm gold grating and a 70 nm gold film on top of the chromium-coated substrate. This fabrication method allowed much larger phase span ($\sim \pm 82\pi$) with respect to the span that is provided by a spatial light modulator.

The experimental setup consists of a Nd:YLF pump laser (1.0475 μm, 3 kHz repetition rate, and 7.62 ns pulse width) which is collimated to waist diameter of 1 mm incident upon the phase mask. The reflected light is then Fourier transformed with a 38 mm lens, thereby generating a parabolic beam at the first diffraction order. This parabolic beam is imaged with 4f system (magnification of 2) into a 10 mm long periodically poled $KTiOPO_4$ (PPKTP) crystal. The nonlinear crystal, with poling period of 8.5 μm, is held at the experimental phase matching temperature of 52.5 ± 0.1 °C. After the crystal, the FH or the SH are filtered and the output beam is imaged with another 4f system (magnification of 3.95) on a CCD camera placed on a rail. Under these conditions, the entire angular spectrum of the beam is within the angular acceptance of the crystal.[26]

We used three different masks to generate 0th, 2nd, and 4th order parabolic beams. Using a FH beam with an average power of 2.5 mW, we measure the SH beam with an average power of 0.016 mW, giving an internal conversion efficiency of 7.75 e-5 W^{-1} (for the peak power), after accounting the Fresnel reflections at the uncoated crystal facets. We then record the output beams after the PPKTP crystal. Since the energy transfer from the FH to the SH is relatively low, the output FH after the crystal essentially remains an undepleted parabolic beam (Figs. 1(d)–1(f)). However, the SH beams (Figs. 1(g)–1(i)) are not pure parabolic beams, though they have some similarity in shape to the FH parabolic beams. We further examine the shape of the SH beams vs. the FH beams. Figs. 2(a)–2(c) present both FH and SH beams on the same figure and two different cross sections (Figs. 2(g)–2(i) and 2(m)–2(o)) along the beams. As can be clearly seen the intensity peaks of the first and second harmonics are asynchronous with one another. The asynchronism in this case, in Cartesian coordinates, lies on the branches of the parabolic axes. This spatial asynchronism was also predicted by numerical simulations (Figs. 2(d)–2(f), 2(j)–2(l) and 2(p)–2(r)). The simulations were done with split step Fourier method with the same conditions as in the experiment and both fit very well. We would like to emphasize that the asynchronism of the first and second harmonics is more complex than in the case of Airy beams since it has a non-orthogonal 2D structure in Cartesian coordinates. By switching to parabolic coordinate system (the dashed lines in Fig. 2) the structural oscillations of the second harmonic at ξ are $2^{2/3} \approx 1.587$ times faster than the structural oscillations in the pump. For η, the faster structural oscillations (for modes n > 0) of the

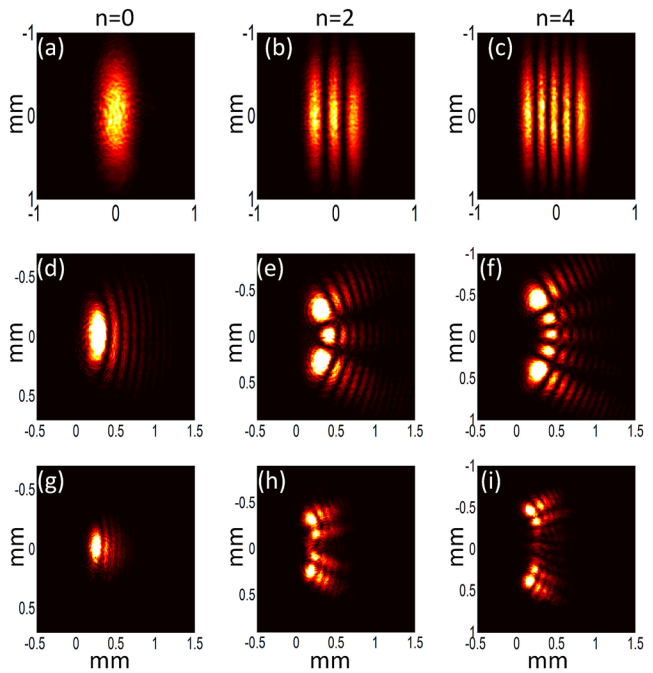

FIG. 1. Experimental results displaying the first harmonic Fourier transform before the nonlinear medium (a)-(c) and the first (d)-(e) and second (g)-(i) harmonic beams after the nonlinear medium for three different modes: n = 0, 2, 4.

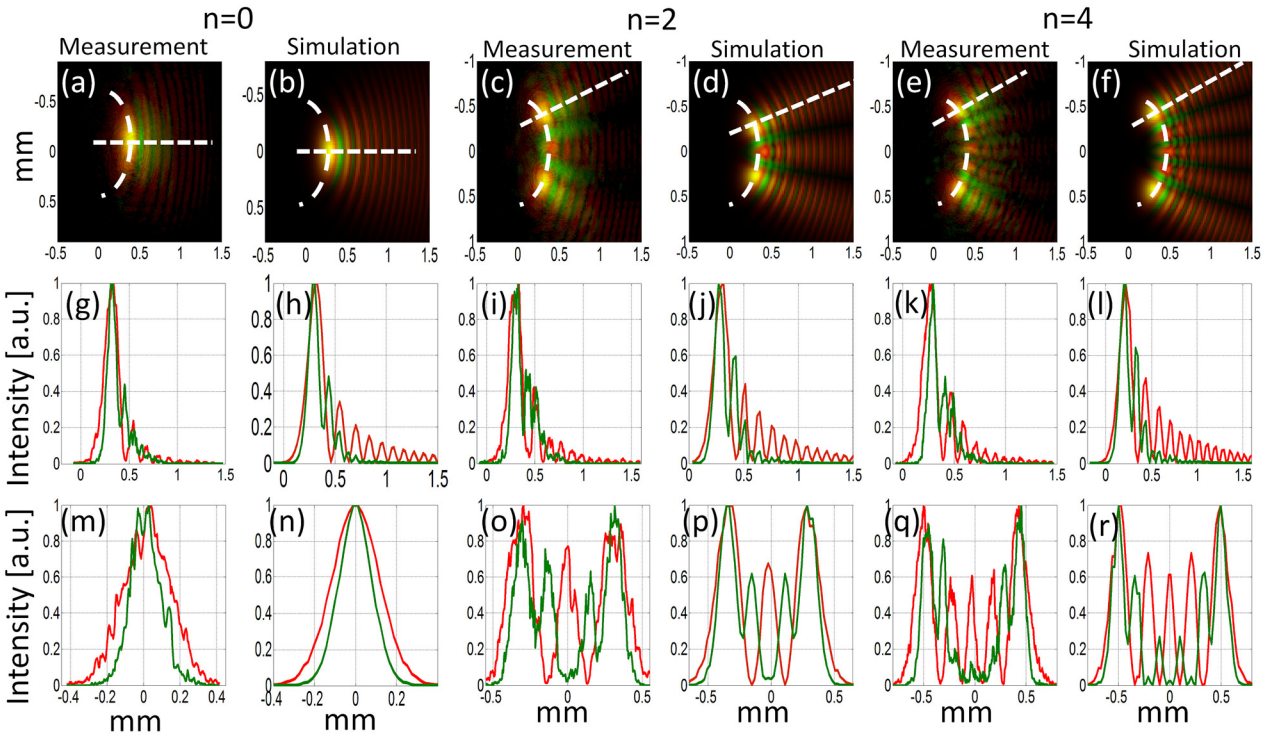

FIG. 2. Experimental and numerical simulations of the parabolic beams measured at the crystal exit face. The combined FH (red) and SH (green) are presented on a log scale (a)-(f), where the dashed lines mark the corresponding cross sections (g)-(r). The curved dashed lines lie along a fixed value of the parabolic coordinate ξ, whereas the straight dashed lines are along a fixed value of η.

second harmonic are completely non-synchronized with the pump, they depend on the order of the parabolic beam n, and typically exhibit one additional lobe. This behavior is significantly different than what was observed for the case of 2D Airy beams,[22] in which $2^{2/3}$ times faster oscillations were observed in both transverse coordinates and it is a proof of concept that these beams exhibit joint-trapping by virtue of the quadratic nonlinearity, in a fashion similar to that supporting quadratic solitons.

Next we measured the acceleration path of the first and second harmonic beams, after the nonlinear crystal, by moving the CCD camera that was placed on a rail. In Figure 3 we present the experimental (Figs 3(a)–3(c)) and simulation (Figs. 3(d)–3(f)) results for the propagation of the fourth order parabolic beam. The first harmonic, which is purely truncated parabolic beam, accelerates on a parabolic path (Fig. 3(g)). The FH and the SH are jointly accelerating, the peaks of the main lobes of the FH and SH accelerate along the same trajectory. We note that a same phenomenon was observed also for the 0th and 2nd order parabolic beams (not presented). We also note that the joint acceleration is directly related to the $2^{2/3} \approx 1.587$ faster oscillations of the second harmonic beam with respect to the fundamental beam: The transverse sizes of the fundamental and second harmonic beams are therefore κ, $\kappa/2^{2/3}$, respectively, whereas the wavevector of the second harmonic is nearly twice as large as that of the fundamental. Therefore, the acceleration of the fundamental beam, $1/(4k^2\kappa^3)$, is nearly identical to that of the second harmonic.

In order to better understand the evolution of accelerating beams inside nonlinear medium, we simulated the buildup and propagation of SH beam inside the nonlinear crystal. Assuming the non-depleted pump approximation the SH beam output shape, after the crystal, is a function only of the normalized interaction length $z/(2k\kappa^2)$. Fig. 4(d) shows the correlation of the SH beam to a theoretical beam for

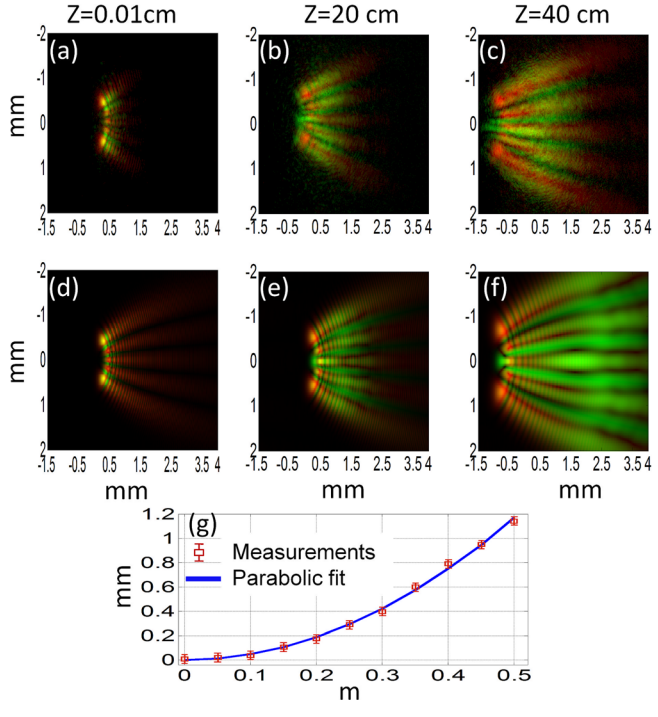

FIG. 3. Acceleration path of the FH (red) and SH (green) beams when a fourth order parabolic beam is launched into the nonlinear crystal. Measurements (a)-(c) and simulation (d)-(f). As shown here, the 2D FH and 2D SH parabolic beams are jointly-accelerating in a parabolic path (g).

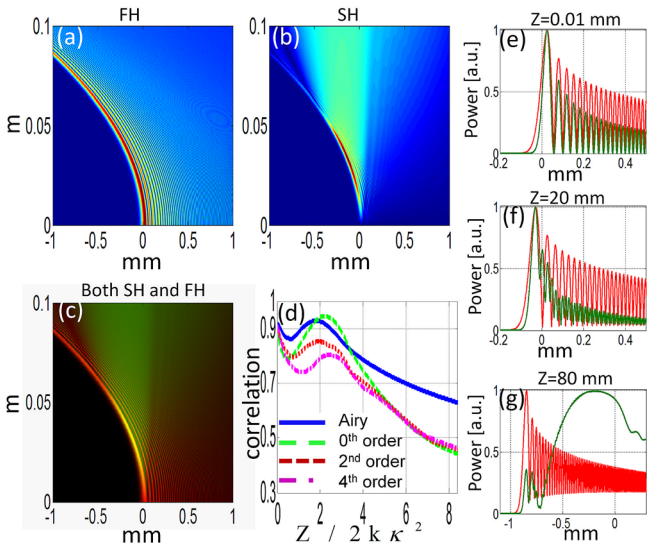

FIG. 4. Simulation of the acceleration path of 1D Airy beam in the nonlinear crystal. FH (a), SH (b), and both (SH and FH). The correlation of the SH beams to theoretical beams for the case of Airy beam and 0th, 2nd, and 4th order parabolic beams (d). Cross sections inside the nonlinear crystal (e)-(g).

parabolic and Airy beams. For correlation higher than 0.80 the normalized interaction length should be less than ~1. When the normalized interaction length is >6 the correlation of the SH to a theoretical beam is less than 0.7. We note that in our experiments the normalized interaction length was less than 0.1, in Ref. 22 it was less than 0.05. When the normalized length is ~7 (Ref. 16), the output SH beam is indeed very different from an Airy beam. To better visualize this effect we present in Fig. 4 a simulation where 1D Airy beam, $\mathrm{Ai}(x/\kappa) \times \exp(-ax/\kappa)$ where $\kappa = 24.8\ \mu$m and $a = 0.01$ (with main lobe full width half maximum of ~57 μm), is launched into a nonlinear crystal. Figs. 4(a) and 4(b) show the evolution of SH and FH inside the nonlinear crystal, respectively, Fig. 4(c) presents both first and second harmonic simultaneously. It can be seen that while the FH maintain its Airy shape while propagating inside the nonlinear crystal the SH beam changes its shape while propagating. Figs. 4(e)–4(g) show different cross section of the beams inside the nonlinear crystal in different locations. From these simulations we see that at the crystal entrance (Fig. 4(e)), the SH beam oscillates at the same rate as the fundamental beam, but after a short propagation distance these oscillations become faster by the known factor of $2^{2/3}$ (Fig. 4(f)), whereas at longer propagation distances, the Gaussian-like part of the beam becomes the dominant part (Fig. 4(g)).

In conclusion, we presented experimental observation of self-accelerating nonlinear parabolic beams in quadratic media. We showed that nonlinearly coupled beams of different frequencies exhibit joint acceleration inside a nonlinear medium which supports their coupling. However, the intensity peaks of the two beams are asynchronous with respect to one another. In parabolic coordinates it can be seen that the oscillations are faster by a rate of $2^{2/3}$ in ξ and in a rate that depends on the parabolic beam order (n) in η. We also demonstrated the impact of the interaction length on the shape of the SH beam. It would be interesting to expand this work to study the nonlinear evolution of other types of self-accelerating beams.[12,13,27] or circular Airy beams.[14] In addition, while our measurements were done at relatively low pump power, accelerating quadratic solitons,[28,29] modulation instability and self-focusing effects could be observed at higher pump powers.

This work was supported by Israel Science Foundation.

[1]M. V. Berry and N. L. Balazs, Am. J. Phys. **47**, 264 (1979).
[2]G. A. Siviloglou and D. N. Christodoulides, Opt. Lett. **32**, 979 (2007).
[3]G. A. Siviloglou, J. Borky, A. Dogariu, and D. N. Christodoulides, Phys. Rev. Lett. **99**, 213901 (2007).
[4]G. A. Siviloglou, J. Borky, A. Dogariu, and D. N. Christodoulides, Opt. Lett. **33**, 207 (2008).
[5]J. Baumgartl, M. Mazilu, and K. Dholakia, Nat. Photonics **2**, 675 (2008).
[6]P. Polynkin, M. Kolesik, J. Moloney, G. A. Siviloglou, and D. N. Christodoulides, Science **324**, 229 (2009).
[7]A. Chong, W. H. Renninger, D. N. Christodoulides, and F. W. Wise, Nat. Photonics **4**, 103 (2010).
[8]D. Abdollahpour, S. Suntsov, D. Papazoglou, and S. Tzortzakis, Phys. Rev. Lett. **105**, 253901 (2010).
[9]G. Porat, I. Dolev, and A. Arie, Opt. Lett. **36**, 4119 (2011).
[10]S. Longhi, Opt. Lett. **36**, 716 (2011).
[11]M. A. Bandres, Opt. Lett. **33**, 1678 (2008).
[12]M. A. Bandres, Opt. Lett. **34**, 3791 (2009).
[13]E. Greenfield, M. Segev, W. Walasik, and O. Raz, Phys. Rev. Lett. **106**, 213902 (2011).
[14]N. K. Efremidis and D. N. Christodoulides, Opt. Lett. **35**, 4045 (2010).
[15]T. Ellenbogen, N. Voloch-bloch, A. Ganany-padowicz, and A. Arie, Nat. Photonics **3**, 395 (2009).
[16]I. Dolev T. Ellenbogen, N. Voloch-bloch, and A. Arie, Appl. Phys. Lett. **95**, 201112 (2009).
[17]I. Dolev, T. Ellenbogen, and A. Arie, Opt. Lett. **35**, 1581 (2010).
[18]I. Dolev and A. Arie, Appl. Phys. Lett. **97**, 170102 (2010).
[19]S. Jia, J. Lee, J. W. Fleischer, G. A. Siviloglou, and D. N. Christodoulides, Phys. Rev. Lett. **104**, 253904 (2010).
[20]Y. Hu, P. Zhang, C. Lou, S. Huang, J. Xu, and Z. Chen, Opt. Lett. **35**, 3952 (2010).
[21]I. Kaminer, M. Segev, and D. N. Christodoulides, Phys. Rev. Lett. **106**, 213903 (2011).
[22]I. Dolev, I. Kaminer, A. Shapira, M. Segev, and A. Arie, Phys. Rev. Lett. **108**, 113903 (2012).
[23]K. Banerjee, S. P. Bhatnagar, V. Choudhry, and S. S. Kanwal, Proc. R. Soc. London, Ser. A **360**, 575–586 (1978).
[24]W. Lee, Appl. Opt. **28**, 3661 (1979).
[25]J. A. Davis, M. J. Mitry, M. A. Bandres, and D. M. Cottrell, Opt. Express **16**, 12866–12871 (2008).
[26]M. M. Fejer, G. A. Magel, D. H. Jundt, and R. L. Byer, IEEE J. Quantum Electron. **28**, 2631–2654 (1992).
[27]I. Kaminer, R. Bekenstein, J. Nemirovsky, and M. Segev, Phys. Rev. Lett. **108**, 163901 (2012).
[28]Y. N. Karamzin and A. P. Sukhorukov, Sov. Phys. JETP **41**, 414 (1976).
[29]W. E. Torruellas, Z. Wang, D. J. Hagan, E. W. VanStyland, and G. I. Stegeman, Phys. Rev. Lett. **74**, 5036 (1995).